Bio-ethylene Production: from Reaction Kinetics to Plant Scale

I. Rossetti*, A. Tripodi*, M. Frosi*, G. Ramis**, N. Mahinpey***
*Chemical Plants and Industrial Chemistry Group, Dip. Chimica, Università degli Studi di Milano, CNR-ISTM and ISTM Unit Milano-Università, Milano, Italy, **Dip. Ing. Chimica, Civile ed Ambientale, Università degli Studi di Genova, Genoa, Italy, *** Dept. of Chemical and Petroleum Engineering, Schulich School of Engineering, University of Calgary, Calgary T2N 1N4, Canada

Abstract

Ethylene production from renewable bio-ethanol has been recently proposed as sustainable alternative to fossil sources. The possibility to exploit diluted bioethanol as less expensive feedstock was studied both experimentally, using different catalysts at lab-level, and through preliminary process design. In this work, a full-scale plant simulation is presented, built on a detailed reaction kinetics. Rate equations for the primary and side reactions are revised and implemented with a process simulation package, using a range of thermodynamic methods as best suited to the different process stages. The catalyst loading within the reactor can be effectively distributed according to the underlying kinetic, and the overall plant layout let foresee the best routes for the material recycles. The detailed reaction modeling and the choice of the thermodynamic models are essential to obtain reliable predictions.
Setting a target yield of 10^5 t/year of polymer-grade ethylene, the reactive section must be fed with 76 t/h of diluted ethanol and operated at 400 °C.
85% of the fed carbon mass is found as ethylene, 12% remains as ethanol and a 2% as longer olefins. Considering also the recycle of ethanol the carbon conversion and recovery increases to the value of 97.6%.
The global ethylene recovery is 90.7%: most of the loss takes place in the last stage due to the non-condensable purification and to the adopted strategy of having low reflux ratio – and then a closed cryogenic balance – in the last purification column.
Full heat integration of the process with upstream bioethanol production and purification sections allows process intensification and consistent energy savings.
This newly designed process sets the sustainable ethylene production on a detailed and reassessed computational basis and has been assessed as for Capital and Operational Expenditures and Total Investment costs.

Introduction

At present, a large part of petrochemical products are produced from ethylene, in addition to its wide usage as monomer for the production of important compounds such as polyethylene, polyvinylchloride and polystyrene. For this reason, ethylene production is considered as one of the indicators to measure the petrochemical development level of countries all over the world.
The main process to obtain ethylene is by hydrocarbons cracking. However, biomass-derived ethanol can be catalytically dehydrated as a sustainable alternative route in order to exploit new renewable sources for ethylene production and decrease the environmental footprint of the process.
The bio-polymer market is continuously growing and the demand for renewable polyethylene corresponds to 10% of the global market, whereas the present supply is less than one-tenth. Therefore, routes to ethylene starting from inexpensive and renewable feedstocks should be explored. A commercial application for ethylene production starting from sugar has already been successfully applied in Brazil (Table 1).

Table 1: Top Industrial Ethylene complexes and their locations ranked by capacity. Reprinted with permission from [1]. Copyright 2019 American Chemical Society.

Data	Company	Location	**Yield (ton/year)**	**Reference**
Plant: Steam cracking	Formosa Plastics	Taiwan	2.7×10^6	[2]
	Nova Chemicals	Canada	2.9×10^6	[3]
	APC	Saudi Arabia	2.2×10^6	[4]
	Exxon Mobile	USA	1.3×10^6	[5]
	Dow DuPont	USA	$1.5 - 2.0 \times 10^6$	[6]
Plant: Bioethanol dehydration	Dow DuPont	Brazil	3.5×10^5	[7]
	Braskem	Brazil	2.0×10^5	[8]
	India Glycols Ltd	India	$<1.7 \times 10^5$	[9]
	Solvay	Brazil	6.0×10^4	[10]
Simulation: Bioethanol dehydration			1.0×10^6	[11]
			2.0×10^5	[12]
			1.8×10^5	[13]

The 13 top industrial ethylene plants and their locations, ranked by capacity are listed in Table 1, where the commercial examples of bioethanol-to-bioethylene plants are also reported.
Bioethanol production plants are an established technology [14–17], now available also from 2nd generation or mixed feedstock [18,19]. On acidic catalysts, *e.g.* zeolites or alumina, ethanol can lose a hydrogen atom turning into ethoxide or dimerize to diethyl ether (or dimerize with the ethoxide itself). Ethylene is likely produced via ether decomposition [20–23].
Fully-integrated plants from bioethanol to polyethylene are usually present, where concentrated ethanol solutions are used [24–26]. This point requires huge energy consumption for the anhydrifcation of ethanol [27], limiting the economic sustainability of ethanol as raw material. However, we have recently demonstrated the possibility to use diluted bioethanol solutions even for this dehydration reaction [1,28–31]. Though there is a thermodynamic penalty, to be overcome by increasing the operating temperature, the savings of energy with respect to the use of anhydrous ethanol is evident.
Based on this idea we have derived a robust kinetic model for the reaction, basing on existing kinetic studies and data [1,32–36]. According to this model we have simulated a full ethanol-to-ethylene plant with detailed separation section, to achieve polymer grade bioethylene.
Based on the designed plant we have optimized the thermal integration of the plant and accomplished a preliminary economic assessment.

Models and methods

Kinetic modelling was done with Matlab® (MathWorks Inc.) scripts.
Plant design and simulation was performed with Aspen Plus® v.8.0 and Aspen Adsorption® (Aspen Tech Inc.). We preliminarily identified the most appropriate thermodynamic models to represent all the fluid properties (by comparison with literature data). They resulted the Non-Random Two-Liquids (NRTL, activity coefficient for liquid phase) coupled to the Redlich-Kwong equation of state (RK, for the vapor phase), Predictive-Redlich-Kwong-Soave (PSRK, equation of state model for both vapor and liquid phases) and Henry pressure-solubility correlation, depending of the plant sections. In addition, the Electrolytes-NRTL (ENRTL) model coupled with the Henry's law was used for the solubility of CO_2 byproduct in water, followed by the first dissociation of carbonic acid.
A Langmuir-Hinshelwood-Hougen-Watson (LHHW) kinetic model was developed through regression of literature data [37].
The model considers the following reactions, which include the reaction enthalpies[38] [12,39,40]:

$C_2H_6O \rightleftarrows C_2H_4 + H_2O$	45 kJ/mol	Direct ethanol dehydration	(1)
$2\ C_2H_6O \rightleftarrows C_4H_{10}O + H_2O$	-12 kJ/mol	Ethanol dimerization	(2)
$C_2H_6O \rightleftarrows C_2H_4O + H_2$	184 kJ/mol	Ethanol dehydrogenation	(3)
$C_4H_{10}O \rightleftarrows 2\ C_2H_4 + H_2O$	115 kJ/mol	Diethyl-ether cracking	(4)
$2\ C_2H_4 \rightleftarrows C_4H_6 + H_2$	-52 kJ/mol	Ethylene dimerization	(5)
$C_2H_6O \rightleftarrows CO + CH_4 + H_2$	49.6 kJ/mol	Ethanol decomposition	(6)
$C_2H_6O + H_2O \rightleftarrows CO_2 + CH_4 + 2H_2$	8.49 kJ/mol	Ethanol decomposition + WGS	(7)

The reaction rates are represented with the general formula (for the molar fractions *y* of every i-th species in the j-th reaction, where the dimensions are carried by the preexponential factor *k*°):

$$r_j = k^0{}_j \left(e^{-E_a/RT}\right) \frac{\prod_i y_i^{\alpha_{i,j}}}{\left(1 + \sum_n K_n \prod_i y_i^{\beta_{i,n}}\right)^{d_j}} \left[\frac{mol}{s \times g_{cat}}\right] \quad (8)$$

The mass and energy balances were then computed through an ideal plug-flow model, without diffusion, leading to the following 1D equations:

$$\frac{\partial n_i}{\partial t} = -u\frac{\partial n_i}{\partial x} + w\sum_j \nu_{ij} r_j = 0 \quad (9)$$

$$\frac{\partial T}{\partial t} = -u\frac{\partial T}{\partial x} + \frac{w}{\bar{C}}\sum_j r_j \Delta H_j = 0 \quad (10)$$

w being the catalyst mass, *u* the gas velocity, $\bar{C}$ the molar heat capacity and *H* the enthalpy). The integration has been carried out with respect to the reactor length *x* by an embedded routine.

Design of an integrated ethanol-to-ethylene plant

The plant flowsheet is reported in Figure 1 and is organized in different blocks.

The reaction section is fed with diluted bioethanol (*e.g.* 40-50 wt% bioethanol as resulting from flash separation of the crude bioethanol beer). The plant was sized to feed 115-170 t/h of 40 vol% bioethanol in water. The products are separated from excess steam and a small amount of unreacted methanol in a flash column. The purification of ethylene is performed at first by CO_2 absorption through washing with alcanolamine (regenerated and recycled in a side column), dehydration through pressure swing adsorption and final rectification with a conventional ethylene purification column.

The detail of the reactive section is instead reported in Fig. 2, where the reactor is split into three adiabatic beds with intermediate heat exchange re-heaters. The product to feed heat exchange is presented in the same Figure, with the detail of heat recovery from the products stream to sustain the separation column and the flash for the recovery of unreacted ethanol.

Figure 1: Plant flowsheet divided into the different blocks. Reprinted with permission from [1]. Copyright 2019 American Chemical Society.

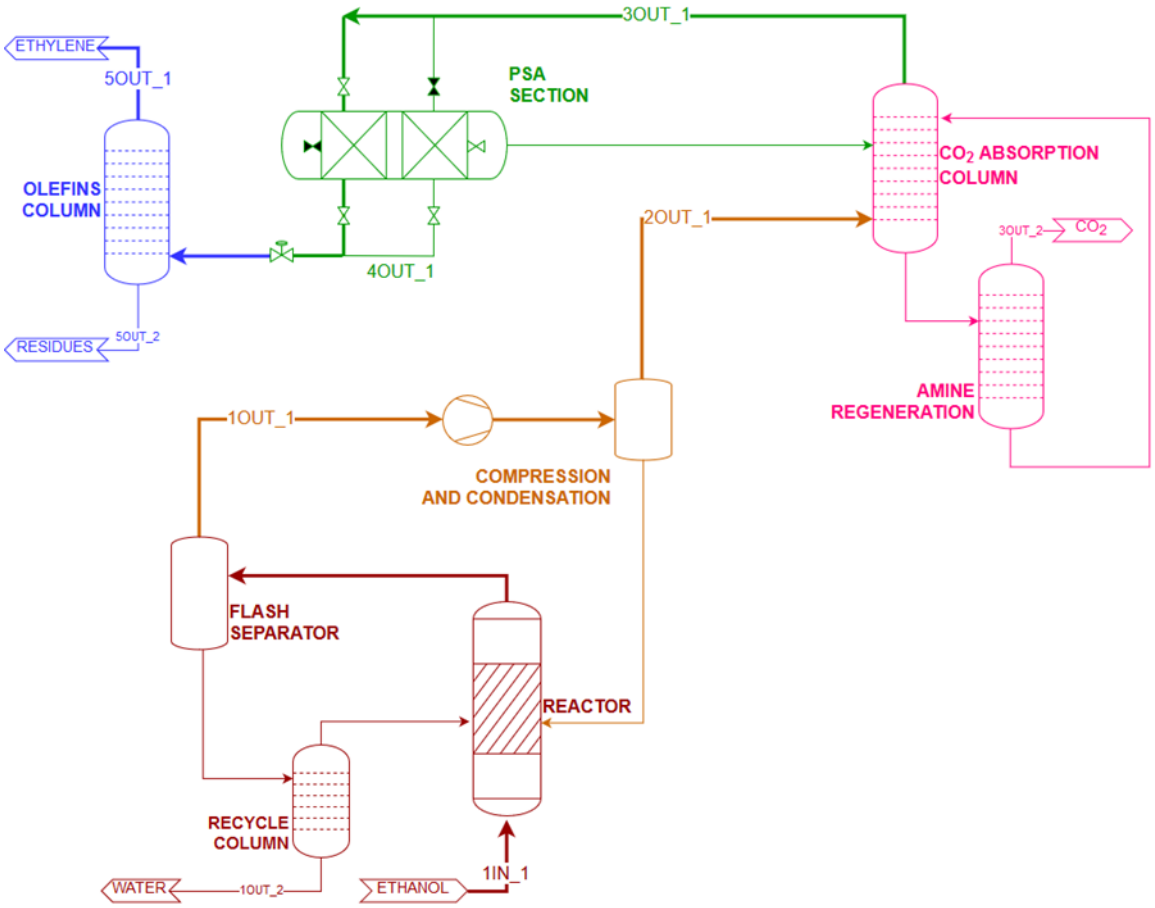

The catalytic beds are based on a commercial alumina catalyst, where the mean temperature is set at *ca.* 400 °C. The inter-bed heaters release the reacting mixture at 430°C to circumvent the excessive cooling in the catalytic bed due to the endothermicity of the reaction.
The first ethylene separation of the product is accomplished with a flash separator where ethylene is recovered as vapor, while most of the water plus unreacted ethanol and polar co-products are found in the liquid phase. The ethanol is then distilled for recycle.
The ethylene line contains excess water, which is mainly discharged through pressurization and phase separation, for instance in a 4-stage compression system, which is depicted in Figure 2 as separate compression-separation systems, but it is conceptually thought as a multistage compressor with intercooling and liquid discharge.
CO_2 (4.4 kg/h) separation is needed to deal with polymer grade ethylene. Its recovery is accomplished by standard scrubbing with an aqueous amine solution [41,42] and the following regeneration and recycle of the base. The two columns are rigorously modelled and thermally integrated with the rest of the plant, since the energy required for the amine regeneration is one of the main items for cost optimization of the system. From the computational point of view this implied a careful selection of the thermodynamic properties package, since the presence of electrolytes induces a strong non-ideality in the mixture, which should be tackled with appropriate models, but introduces complexity in the simulation. The selected models, thanks to literature survey and comparison with available experimental data, were the ENRTL one for the calculation of activity coefficients in the liquid phase and the Redlick Kwong equation of state for the gas phase. The selected amine was the N-Methyldiethanolamine (MDA).
Figure 2: Ethylene reactor with water condensation and ethanol recovery (left), and compression with further water separation (right). Reprinted with permission from [1]. Copyright 2019 American Chemical Society.

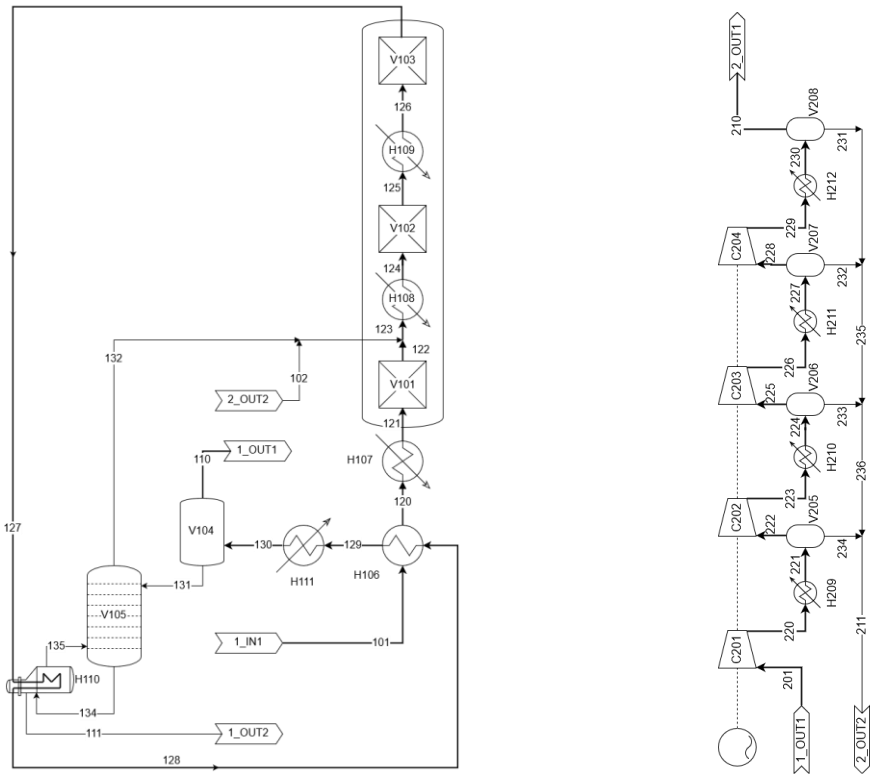

Residual water in the ethylene stream is finally removed through pressure-swing adsorption (PSA) on zeolites. This system is quite established and well fits the stream conditions, since this part of the plant has sufficiently high pressure to allow its exploitation in a PSA system.
A series of 2 adsorption beds, operating alternatively in a 4-step cycle is designed [1], which are regenerated with a fraction of the dry ethylene, to avoid the addition of new pressurized gas lines. This approach is also common for similar ethanol dehydration layouts [43,44].
Pressure difference was set from 5 to 1 bar, with 2 mol% water content. This implies the creation of a new recycle loop, where the humid ethylene from regeneration is *ca*. 50% of the fresh incoming stream (22 ton/h for a nominal plant size of 45 ton/h of dry ethylene). The recycle loop needs recompression and cooling before feeding the CO_2 absorbing column at 15 atm and 20 °C.
Possible byproducts of the reaction include heavier olefins, such as dimers (butane, butylene), or, depending on reaction conditions, a mixture C4, C6 and heavier products (even aromatics) can be obtained [45].
The cryogenic ethylene purification is then needed, here modelled considering butylene as model byproduct, at 5 atm as the PSA unit.
The overall mass balance of the plant concludes that 85% of the fed carbon mass is found as ethylene, 12% remains as ethanol, to be recycled, and a 2% as higher olefins. Including the ethanol recycle the carbon conversion raises to 97.6% with 90.7% ethylene recovery. The main loss is in the last column due to its low reflux ratio.
The final ethylene purity has been set to 99.96% with 0.022% of lighter and 0.017% heavier impurities.

Preliminary economic assessment

A preliminary economic analysis was carried out assuming 8406 h/year (96%) of operating hours, 20 years of plant life and 10 years of payback time. A first estimate of energy integration was accomplished through the Aspen Energy Analyzer®. This allowed energy savings from 14 to 53%, through rigorous design of the heat exchangers, while adopting various hot/cold stream integrations.
The Aspen Economic Analyzer® was then used, with state of the art selection of equipment and materials for construction. All of the equipment costs were actualized using the CEPC

index [46], considering CEPCI in January 2016 = 536.5, increasing by 3.1% to January 2017, by 4.2% to January 2018 and 7.4% by January 2019 (*i.e*. = 544.42 in 2019). All the costs reported in the following were actualized in this way.
Being specified as adiabatic, the reactors could not be sized by varying the length and, thus, the conversion. In the original papers [35,47], a residence time between 2 and 4 s was indicated to achieve the desired conversion. From these data, a length of 4 m and a diameter of 1 m was set. The reactor was specified as a multitubular reactor with 100 tubes. To each or the three reaction blocks was attributed a cost of 277,334 USD.
The flash drum separators were sized and their cost ranged between 645,000 USD to 1,536,655 USD, depending on the flowrate to be treated and the relative size.
For the columns the Standard-Total configuration was chosen that was comprehensive of a tray tower (specified tray tower with single diameter), the condenser, the condenser accumulation drum, the reflux pump, the overhead split, the bottom split and the reboiler. The cost for each column tanged between 700,000 and 920,000 USD.
Centrifugal single or multi-stage pumps (cost ranging between 70,000 and 100,000 USD), centrifugal horizontal compressors (cost ranging between 1 and 10 million USD) and static mixers (cost ranging between 36,000 and 4 million USD) were chosen.
The PSA unit was filled with 13X zeolite and after sizing it showed a cost for 2 columns of 26,000 USD.
Heat exchangers were rigorously sized, with different configuration and passes depending on the case. Their cost was widely variable depending on the case of heat integration selected.
A preliminary economic evaluation was carried out as total manufacturing expenses, calculated from the sum of Capital Expenses (capital investment) and Operating Expenses. From the total expenses, the net annual profit is derived, together with the Cash Flow analysis.
The non-heat-integrated process was first analysed, showing a total equipment cost of 54 Million USD, from which a total capital investment of 285 million USD was calculated.
The total manufacturing expenses was estimated as 326 million USD. The net revenues from sales was 445 Million USD with an annual net profit after taxes of 124 million USD.
The price of bioethylene at which the Net Present Value of the plant is equal to zero is 0.90 USD/kg. Further options including different arrangements for heat integration will be compared with this solution.

Conclusions

A newly designed ethanol to ethylene production plant is designed, employing diluted bioethanol as feed (40 vol%). The plant includes a multitubular three bed reactor, with inter-heating, a section for the separation of excess water and ethanol recycle, a full purification train for bioethylene.
Different possible heat integration options have been checked
A preliminary economic assessment allowed to identify the total capital investments and the main remuneration parameters, to be further optimized after the optimization of the heat exchange network.

References

[1] Tripodi A, Belotti M, Rossetti I. Bioethylene Production: From Reaction Kinetics to Plant Design. ACS Sustain Chem Eng 2019;7:13333–50. doi:10.1021/acssuschemeng.9b02579.

[2] “Plant Status: Taiwan’s Formosa Plastics,” ICIS News, 2019. [Online]. Available: https://www.icis.com/explore/resources/news/2019/02/12/10317435/plant-status-taiwan-s-formosa-plastics-to-shut-eva-plant-on-18-feb/. [Accessed: 23-Apr-2019]. ICIS News 2019.

[3] “Nova Plant facilities,” Nova Chemicals. [Online]. Available: http://www.novachem.com/Pages/joffre/joffre-plants.aspx. [Accessed: 23-Apr-2019]. Nov Chem n.d.

[4] Fan D, Dai DJ, Wu HS. Ethylene formation by catalytic dehydration of ethanol with industrial considerations. Materials (Basel) 2013;6:101–15. doi:10.3390/ma6010101.

[5] “Exxon Mobile Starts Up New ethane cracker in Baytown, TX,” 2018. [Online]. Available: https://news.exxonmobil.com/press-release/exxonmobil-starts-new-ethane-cracker-baytown-texas. [Accessed: 23-Apr-2019] 2018.

[6] Erpelding J. J. Erpelding, “DowDuPont announces start-up of world-scale ethylene production facility,” The Dow Chemical Company, 2017. [Online]. Available: https://corporate.dow.com/en-us/news/press-releases/dow-announces-startup-of-worldscale-ethylene-production-faci. Dow Chem Co 2017.

[7] Tullo A. “Notes On Dow’s Brazilian Biopolymers Project,” 2011. [Online]. Available: http://cenblog.org/the-chemical-notebook/2011/07/447/. [Accessed: 23-Apr-2019]. 2011.

[8] “I’m Green Polyethylene.” [Online]. Available: http://plasticoverde.braskem.com.br/site.aspx/Im-greenTM-Polyethylene. [Accessed: 23-Apr-2019] n.d.

[9] Broeren M. “Production of Bio-ethylene,” IEA-ETSAP and IRENA, no. January, pp. 1–9, 2013. IEA-ETSAP and IRENA 2013:1–9.

[10] Tardy M. “SOLVAY INDUPA WILL PRODUCE BIOETHANOL-BASED VINYL IN BRASIL,” Solvay press release, https://www.chemeurope.com/en/news/75840/solvay-indupa-will-produce-bioethanol-based-vinyl-in-brasil-considers-state-of-the-art-power-generation-in-argentina.html. 2007.

[11] Le L, Nagulapalli N, Cameron G, Levine J. Process Design for the Production of Ethylene from Ethanol. Sr Des Reports 2012;39:1–144.

[12] Arvidsson M, BJORN L. Process integration study of a biorefinery producing ethylene from lignocellulosic feedstock for a chemical cluster. Chalmers University of Technology, Goteborg (SE), 2011.

[13] Mohsenzadeh A, Zamani A, Taherzadeh MJ. Bioethylene Production from Ethanol : A Review and Techno-economical Evaluation. ChemBio Eng Rev 2017:75–91. doi:10.1002/cben.201600025.

[14] Zabed H, Sahu JN, Suely A, Boyce AN, Faruq G. Bioethanol production from renewable sources: Current perspectives and technological progress. Renew Sustain Energy Rev 2017;71:475–501. doi:10.1016/j.rser.2016.12.076.

[15] Liptow C, Tillman AM, Janssen M, Wallberg O, Taylor GA. Ethylene based on woody biomass - What are environmental key issues of a possible future Swedish production on industrial scale. Int J Life Cycle Assess 2013;18:1071–81. doi:10.1007/s11367-013-0564-6.

[16] Muñoz I, Flury K, Jungbluth N, Rigarlsford G, I Canals LM, King H. Life cycle assessment of bio-based ethanol produced from different agricultural feedstocks. Int J Life Cycle Assess 2014;19:109–19. doi:10.1007/s11367-013-0613-1.

[17] Vohra M, Manwar J, Manmode R, Padgilwar S, Patil S. Bioethanol production: Feedstock and current technologies. J Environ Chem Eng 2014;2:573–84. doi:10.1016/j.jece.2013.10.013.

[18] Aditiya HB, Mahlia TMI, Chong WT, Nur H, Sebayang AH. Second generation bioethanol production: A critical review. Renew Sustain Energy Rev 2016;66:631–53. doi:10.1016/j.rser.2016.07.015.

[19] Lennartsson PR, Erlandsson P, Taherzadeh MJ. Integration of the first and second generation bioethanol processes and the importance of by-products. Bioresour Technol 2014;165:3–8. doi:10.1016/j.biortech.2014.01.127.

[20] Knaeble W, Iglesia E. Kinetic and Theoretical Insights into the Mechanism of Alkanol Dehydration on Solid Brønsted Acid Catalysts. J Phys Chem C 2016;120:3371–3389. doi:10.1021/acs.jpcc.5b11127.

[21] Alexopoulos K, John M, Borght K Van Der, Galvita V, Reyniers M, Marin GB. DFT-based microkinetic modeling of ethanol dehydration in H-ZSM-5. J Catal 2016;339:173–85. doi:10.1016/j.jcat.2016.04.020.

[22] DeWilde JF, Chiang H, Hickman DA, Ho CR, Bhan A. Kinetics and mechanism of ethanol dehydration on Al 2O3: The critical role of dimer inhibition. ACS Catal 2013;3:798–807. doi:10.1021/cs400051k.

[23] Christiansen M a., Mpourmpakis G, Vlachos DG. DFT-driven multi-site microkinetic modeling of ethanol conversion to ethylene and diethyl ether on γ-Al2O3(111). J Catal 2015;323:121–31. doi:10.1016/j.jcat.2014.12.024.

[24] Cook D, Hodge S, Moffatt C. Ethanol-to-ethylene process provides alternative pathway to plastics. Hydrocarb Process 2014;July:https://www.hydrocarbonprocessing.com/magazine/201.

[25] Jernberg J, Nørregård Ø, Olofsson M, Persson O, Thulin M, Hulteberg C, et al. Ethanol Dehydration to Green Ethylene 2015.

[26] Ethylene from Ethanol, Chematur Engineering AB n.d. https://chematur.se/technologies/bio-chemicals/bio-ethylene-ethene/.

[27] Rossetti I, Lasso J, Compagnoni M, De Guido G, Pellegrini L. H2 production from bioethanol and its use in fuel-cells. Chem Eng Trans 2015;43:229–34.

doi:10.3303/CET1543039.

[28] Rossetti I, Compagnoni M, Finocchio E, Ramis G, Di Michele A, Millot Y, et al. Ethylene production via catalytic dehydration of diluted bioethanol: a step towards an integrated biorefinery. Appl Catal B Environ 2017;210:407–20.

[29] Rossetti I, Tripodi A, Bahadori E, Ramis G. Exploiting Diluted Bioethanol Solutions for the Production of Ethylene : Preliminary Process Design and Heat Integration. Chem Eng Trans 2018;65:73–8. doi:10.3303/CET1865013.

[30] Rossetti I, Compagnoni M, De Guido G, Pellegrini L, Ramis G, Dzwigaj S. Ethylene production from diluted bioethanol solutions. Canad J Chem Eng 2017;95:1752.

[31] Ramis G, Rossetti I, Tripodi A, Compagnoni M. Diluted bioethanol solutions for the production of hydrogen and ethylene. vol. 57. 2017. doi:10.3303/CET1757278.

[32] Tripodi A, Compagnoni M, Martinazzo R, Ramis G, Rossetti I. Process Simulation for the Design and Scale Up of Heterogeneous Catalytic Process: Kinetic Modelling Issues. Catalysts 2017;7. doi:10.3390/catal7050159.

[33] Kang M, Bhan A. Kinetics and mechanisms of alcohol dehydration pathways on alumina. Catal Sci Technol 2016;6:6667–78. doi:10.1039/C6CY00990E.

[34] Lee J, Szany J, Kwak JH. Ethanol dehydration on g-Al2O3: Effects of Partial Pressure and Temperature. Mol Catal 2017;434:39–48.

[35] Maia JGSS, Demuner RB, Secchi AR, Melo PA, Carmo RW Do, Gusmão GS. Process Modeling and Simulation of an Industrial-Scale Plant for Green Ethylene Production. Ind Eng Chem Res 2018;57:6401–16. doi:10.1021/acs.iecr.8b00776.

[36] Becerra J, Quiroga E, Tello E, Figueredo M, Cobo M. Kinetic modeling of polymer-grade ethylene production by diluted ethanol dehydration over H-ZSM-5 for industrial design. J Environ Chem Eng 2018;6:6165–74. doi:10.1016/j.jece.2018.09.035.

[37] Kagyrmanova AP, Chumachenko VA, Korotkikh VN, Kashkin VN, Noskov AS. Catalytic dehydration of bioethanol to ethylene: Pilot-scale studies and process simulation. Chem Eng J 2011;176–177:188–94. doi:10.1016/j.cej.2011.06.049.

[38] Yakovleva IS, Banzaraktsaeva SP, Ovchinnikova E V., Chumachenko VA, Isupova LA. Catalytic Dehydration of Bioethanol to Ethylene. Review. Katal v Promyshlennosti 2016;16:57–73. doi:10.18412/1816-0387-2016-1-57-73.

[39] Skinner MJ, Michor EL, Fan W, Tsapatsis M, Bhan A, Schmidt LD. Ethanol dehydration to ethylene in a stratified autothermal millisecond reactor. ChemSusChem 2011;4:1151–6. doi:10.1002/cssc.201100026.

[40] Kochar NK, Merims R, Padia AS. Ethylene from Ethanol. Chem Eng Process 1981;77:66–70.

[41] de Guido G, Compagnoni M, Pellegrini LA, Rossetti I. Mature versus emerging technologies for CO2 capture in power plants: Key open issues in post-combustion amine scrubbing and in chemical looping combustion. Front Chem Sci Eng 2018. doi:10.1007/s11705-017-1698-z.

[42] Rufford TE, Smart S, Watson GCY, Graham BF, Boxall J, Diniz da Costa JC, et al. The removal of CO2 and N2 from natural gas: A review of conventional and emerging process technologies. J Pet Sci Eng 2012;94–95:123–54. doi:10.1016/j.petrol.2012.06.016.

[43] Simo M, Brown CJ, Hlavacek V. Simulation of pressure swing adsorption in fuel ethanol production process. Comput Chem Eng 2008;32:1635–49. doi:10.1016/j.compchemeng.2007.07.011.

[44] Aden a, Ruth M, Ibsen K, Jechura J, Neeves K, Sheehan J, et al. Lignocellulosic Biomass to Ethanol Process Design and Economics Utilizing Co-Current Dilute Acid Prehydrolysis and Enzymatic Hydrolysis for Corn Stover. Natl Renew Energy Lab 2002:Medium: ED; Size: 154 pages. doi:NREL/TP-510-32438.

[45] Phung TK, Radikapratama R, Garbarino G, Lagazzo A, Riani P, Busca G. Tuning of product selectivity in the conversion of ethanol to hydrocarbons over H-ZSM-5 based zeolite catalysts. Fuel Process Technol 2015;3. doi:10.1016/j.fuproc.2015.03.012.

[46] www.chemengonline.com n.d.

[47] Maia JGSS, Demuner RB, Secchi AR, Biscaia EC. Modeling and simulation of the process of dehydration of bioethanol to ethylene. Brazilian J Chem Eng 2016;33:479–90. doi:10.1590/0104-6632.20160333s20150139.